IEEE Access
Multidisciplinary | Rapid Review | Open Access Journal

SPECIAL SECTION ON NEW TRENDS IN BRAIN SIGNAL PROCESSING AND ANALYSIS

Received January 31, 2019, accepted February 14, 2019, date of publication February 22, 2019, date of current version March 18, 2019.

Digital Object Identifier 10.1109/ACCESS.2019.2901055

Automated Categorization of Multi-Class Brain Abnormalities Using Decomposition Techniques With MRI Images: A Comparative Study

ANJAN GUDIGAR[1], U. RAGHAVENDRA[1], EDWARD J. CIACCIO[2], N. ARUNKUMAR[3], ENAS ABDULHAY[4], AND U. RAJENDRA ACHARYA[5,6,7]

[1]Department of Instrumentation and Control Engineering, Manipal Institute of Technology, Manipal Academy of Higher Education, Manipal 576104, India
[2]Department of Medicine, Columbia University, New York, NY 10032, USA
[3]Department of Electronics and Instrumentation, SASTRA University, Thanjavur 613401, India
[4]Department of Biomedical Engineering, Faculty of Engineering, Jordan University of Science and Technology, Irbid 22110, Jordan
[5]Department of Electronics and Computer Engineering, Ngee Ann Polytechnic, Singapore 599489
[6]Department of Biomedical Engineering, School of Science and Technology, SUSS University, Singapore 599491
[7]School of Medicine, Faculty of Health and Medical Sciences, Taylor's University, Subang Jaya 47500, Malaysia

Corresponding author: Enas Abdulhay (ewabdulhay@just.edu.jo)

ABSTRACT Medical imaging and analysis are useful to visualize anatomic structure. However, analysis of the pathologic substrate is difficult and inefficient when using simple imaging tools. The manual detection and classification of brain abnormality is particularly tedious. Moreover, the currently used methodology suffers from interobserver variability during image interpretation. Magnetic resonance imaging (MRI) is an efficient imaging technique for revealing complex anatomical architecture, and it is highly efficacious for precise brain imaging. Herein, we describe a novel computer aided diagnosis method for automated processing of brain MRI images. The performances of two decomposition techniques, namely, bidimensional empirical mode decomposition and variational mode decomposition (VMD), are compared. Thereafter, bispectral feature extraction and supervised neighborhood projection embedding are implemented to represent each feature in a new subspace, for the automated classification of various categories of disease. A support vector machine classifier is used to train and test the performance accuracy. The level of classification accuracy of 90.68%, 99.43% sensitivity and 87.95% specificity is obtained using the VMD technique. Hence, the developed system can be used as an adjunct tool by radiologists to confirm their screening.

INDEX TERMS Bispectral feature, brain pathology, neighborhood projection embedding, support vector machine, variational mode decomposition.

I. INTRODUCTION

One of the largest and most complex organs in the human body is the brain, which is contained in the skull of vertebrates, and it functions as the control center for sensation, and intellectual and nervous activity. The brain acts automatically and rapidly when it is healthy. Disorders of the center of the nervous system can simply be characterized as brain disease. Brain disease can be categorized into four types: cerebrovascular: It refers to an assembly of conditions which affects blood supply to the brain, degenerative: It is a process which results in change in cells, effects organs or tissues, neoplastic: It is a condition which supports tumor growth inside the brain, and infectious: It is a group of diseases created by organisms [1]. Currently, diagnosis of brain disease has been on the increase worldwide. It can affect individuals at any age. Early detection is assistive to maintain a healthy lifestyle through currently available treatment modalities. Medical imaging produces a visual depiction of the interior substrate, and it is highly assistive for diagnostic purposes. Magnetic resonance imaging (MRI), computed tomography (CT), and positron emission tomography (PET) are ubiquitous imaging techniques. MRI lacks ionizing-radiation hazard, it is fast, and it is a non-invasive imaging technique [2], [3]. The visibility of brain, soft-tissues, nerves, ligaments, and muscles are often clearer via MRI as compared to CT and X-ray analysis [3]. Hence, it is typically used in clinics and hospital settings for medical diagnosis.

The associate editor coordinating the review of this manuscript and approving it for publication was Victor Hugo Albuquerque.

In recent years, computer aided diagnosis (CAD) has become an important research topic, as it has the capability to improve medical diagnostics. CAD combines medical expertise with computational means. Computerized output can serve as a decision verification tool for the radiologist [4], [5], [73]–[76]. In the past decade, investigators have suggested pathological brain detection approaches using MRI images. Often, the discrete wavelet transform (DWT) is incorporated by researchers with the Haar and Daubechies-4 wavelets. In [2], DWT is used for classification. Both self-organizing maps (SOM) and the support vector machine (SVM) are applied to obtain an accuracy of 94% and 98%, respectively. Accuracies of 95.7% and 98.6% were obtained using the feed-forward back propagation artificial neural network (ANN) and k-nearest neighbor (k-NN) classifiers. They have used DWT with Haar for feature extraction, followed by data reduction via principal component analysis (PCA) [6]. In [7], a neural network based normal versus abnormal classification method was proposed; it achieved 100% accuracy with only 66 input images used for training. DWT was utilized in combination with PCA based features and an adaptive chaotic particle swarm optimization (ACPSO) [8], with a scaled chaotic artificial bee colony (SC-ABC) [9], with kernel SVM (KSVM) [10], and with PSO-KSVM [11]. PCA in combination with linear discriminant analysis (LDA) has also been used with DWT, and reached a 99.22% accuracy level with a random forest classifier for dataset-255 [12]. In [13], the stationary wavelet transform (SWT) and PCA were combined with a generalized eigenvalue proximal SVM (GEPSVM) and RBF kernel, to obtain a maximum accuracy of 99.41% for dataset-255. Authors have proposed various CAD tools using the ripplet transform [14], fractional Fourier entropy (FFE) [15], and the dual-tree complex wavelet transform (DTCWT) [16]. To select features, Welch's t-test can be employed [15]. In [16], GEPSVM and twin SVM classifiers were combined with variance and entropy (VE) to achieve an accuracy of 99.57% using twin SVM. Use of FFE and adaptive real-coded biogeography-based optimization (ARCBBO) with multi-layer perceptron (MLP) has also been proposed [17]. Classification techniques such as the naive Bayes classifier [18], fuzzy SVM [19], and AdaBoost with random forest (ADBRF) [20] were also implemented in prior studies. In [20], a probabilistic PCA is used, which improves classification accuracy as compared to PCA. Features such as entropy [15]–[17], [19], [21], energy, and variance [21], a scale invariant feature transform and histogram of oriented gradient [22], and the gray-level co-occurrence matrix [23], [24] are also described for brain abnormality detection. The fast discrete curvelet transform (FDCT) features are extracted and feature size is reduced using PCA, followed by a least-squares SVM implementation for classification [25]. In [26], a reduced feature set using PCA + LDA was classified using a combination of modified differential evolution (MDE) and extreme learning machine (ELM) algorithms. The same research group has used the discrete ripplet-II transform and a combined modified PSO and ELM for segregation tasks [27]. In [77], pseudo zernike moment and kernel SVM is used to achieve an accuracy of 99.45 $\pm$ 0.38%. Recently, a large brain MRI dataset has been analyzed [28]. The authors made a comparative study based upon a multiresolution analysis, and achieved a satisfactory result for the combination of shearlet transform (ST) with PSO-SVM. Since deep learning is attractive methodology in recent years, the convolutional neural network (CNN) is proposed by the authors. The model such as AlexNet [78] and ResNet34 [79] are used to achieve the highest accuracy of 100%. However, in [80] the attempt of multi-class categorization of brain pathology was made by considering total image of 200 and achieved 93% for multi-class dataset by extracting entropy over curvelet subbands (i.e., FCEntF-I and FCEntF-II).

In most published works, the authors have proposed segregation of brain MRI into normal versus abnormal (two-class problem). The dataset typically used for brain image analysis consists of datasets D: 66 (normal: 18, abnormal: 48), D: 160 (normal: 20, abnormal: 140), D: 255 (normal: 35, abnormal: 220), and D: S (different normal and abnormal count). Many methods have been proposed for improved classification accuracy, which has reached approximately 100%. From the literature, it is evident that promising results have been achieved by considering brain pathology identification as two-class classification problem. The existing approaches using handcrafted features and CNNs have attained a promising result for the identification of normal and abnormal cases. However, a multi-class categorization with a greater input pool of varying images could be highly efficacious to improve diagnostics. Hence there is a scope to improve the existing approach into a multi-class categorization problem.

In this respect, the goals of our study were three-fold:

- Generation of efficient descriptors to address nonlinearity in brain anatomy, using spectral features.
- Understanding the data distribution of brain pathology by using embedded graphs and labeling information.
- Use of a large dataset, considering differing types of brain pathology as distinct classes.

II. FRAMEWORK OF THE PROPOSED METHODOLOGY

Healthy brain MRI, and pathological brain MRI belonging to several categories, were used for analysis in this study. The image dimension is 256×256 pixels, the MRI mode is T2-weighted, and the data were acquired along the axial plane. The images are available from the Harvard Medical School Database: http://www.med.harvard.edu/AANLIB/. The brain disease categories were: cerebrovascular, neoplastic, degenerative and inflammatory. A total of 612 images were analyzed: 83 normal, 187 cerebrovascular, 96 neoplastic, 132 degenerative and 114 inflammatory. A detailed description of the dataset used can be found in [28]. Examples of brain MRI are portrayed in Figure 1. The categories of brain disease were treated as a multi-class categorization task.

Figure 2 depicts an overview of the proposed pipeline structure to categorize multi-class brain MRI. It consists of

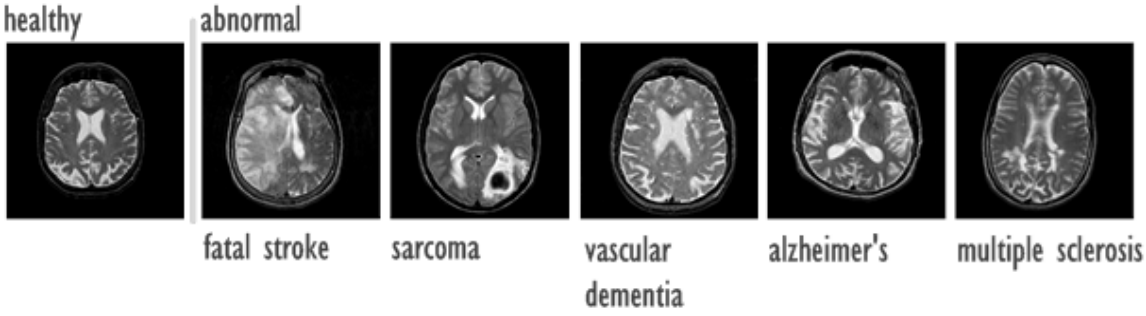

FIGURE 1. Samples of various brain MRI images.

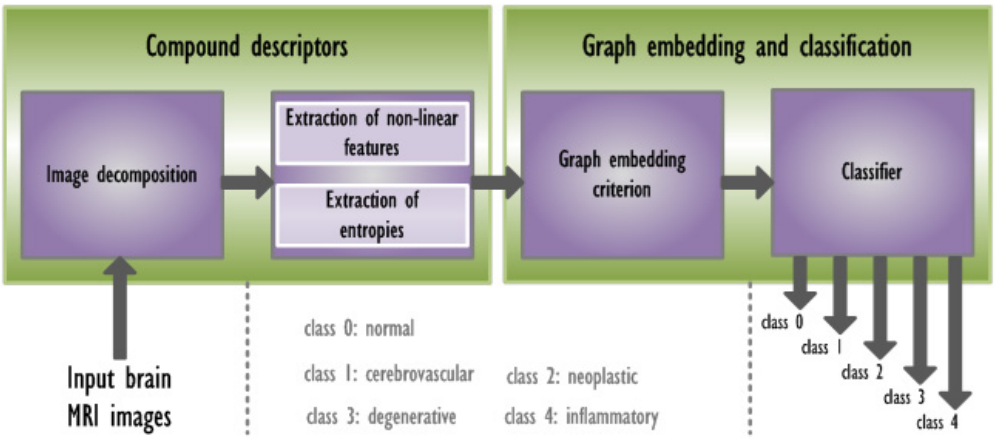

FIGURE 2. Outline of the proposed pipeline architecture.

stages for generation consisting of a compound descriptor, graph embedding, and classification. We adaptively decomposed brain MRI and their spectral information using the bispectrum method, and evaluation was done to determine the presence of nonlinearity. The extracted spectral and entropy features were pooled together to form a compound descriptor. The underlying nonlinear data structure was detected with a graph embedding criterion. A supervised neighborhood preserving embedding (SNPE) was incorporated, thus creating a projection space for 5 classes. Finally, the class label was predicted using machine learning algorithms to identify brain abnormality. For statistical evaluation, the dataset was randomly partitioned into ten training-testing sets.

A. EXTRACTION OF COMPOUND DESCRIPTORS

The generation of compound features is shown in Figure 3, which includes three sequential steps i.e.: 1) image decomposition, 2) extraction of spectral features and entropy, and 3) feature appending.

1) IMAGE DECOMPOSITION

Generally, decomposition of digital images in various spectral bands provides unique patterns and can act to contract redundant information. Bidimensional empirical mode decomposition (BEMD) and variational mode decomposition (VMD) are used for this purpose.

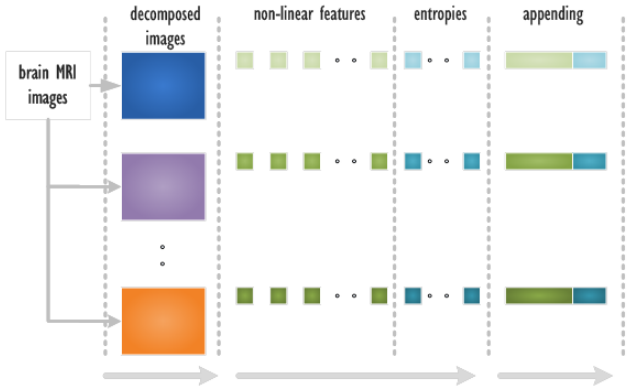

FIGURE 3. Generation of compound features.

Bidimensional empirical mode decomposition

BEMD is the 2D extension of empirical mode decomposition. BEMD finds image local extrema points and estimates the lower and upper envelope of the data by interpolation [29]. Hence, image components are extracted in various frequency bands. BEMD decomposes the image into bidimensional intrinsic mode functions (IMFs) and a bidimensional

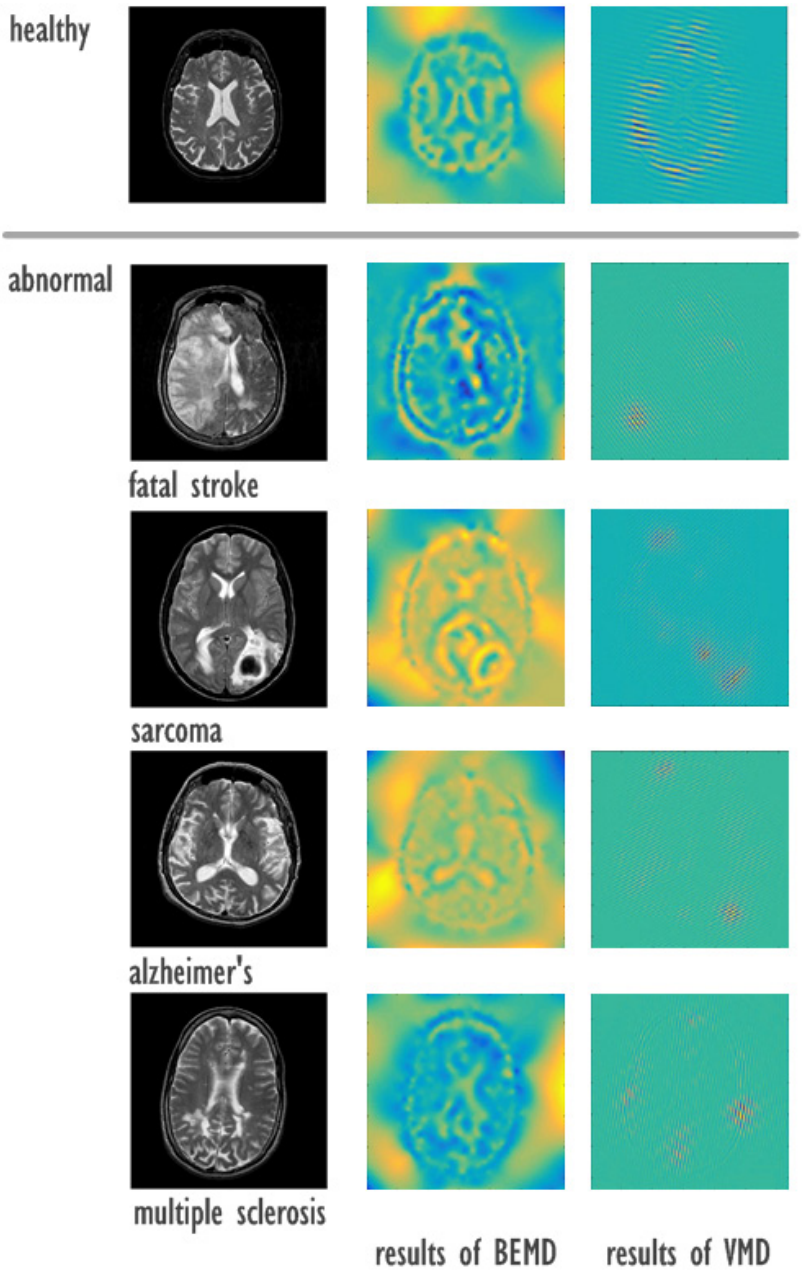

FIGURE 4. BEMD (IMF2) and VMD coefficients of normal and abnormal classes.

residue (RES), which subsequently provide the higher and lower frequency components, respectively. These components are generated using a sifting process. The result of BEMD for healthy and diseased brain MRI inputs are shown in Figure 4. It results in the components IMF1, IMF2, IMF3 and RES, i.e., three IMF components and one residue [30].

Variational Mode Decomposition

2D-VMD is an adaptive and non-recursive technique for sparse image decomposition with minimal parameters [31]. The 1D-VMD is adapted to two-dimensions, which is suitable for image analysis. In 1D the negative frequencies are suppressed in order to obtain the analytic signal, while in 2D one half-plane must be set to zero in the frequency domain. Furthermore, the analytic signal can be defined using its Fourier property, as described in [32]. 2D-VMD for healthy and diseased brain MRIs are shown in Figure 4, while keeping the number of modes at 5.

2) FEATURES EXTRACTION

Higher-order spectral analysis (HOS) is a technique useful for improved spectral representation of images, and finds wide application in pattern recognition and medical image analysis [33]–[35]. In the time domain, HOS is related to

the higher-order moments of the signal [36]. Generally, the bispectrum of the 1D discrete signal is the 3rd order spectrum, which is 2D in nature (i.e., (f_1, f_2)), if $f_2 = 0$, then $B(f_1, 0)$ is a power spectrum. Unlike the power spectrum (i.e., related to signal variance), HOS provides additional insight concerning signal statistics. In particular, the bispectrum of a 2D signal is 4D, and the original image can be reduced to a set of 1D scalar functions using the Radon transform (RT) [37], [38]. The RT performs a successive projection at an angle θ (in this work every 10° of rotation is considered). For every resultant 1D function the bispectrum is computed. Differently configured bispectral features are extracted from the bispectrum plot, for example the normalized 1st, 2nd, and 3rd bispectral entropies. Furthermore, the bispectrum plot orientation is analyzed by computing its phase entropy [34], [39]. As a result, a total of $18 \times 4 = 72$ features are calculated for a single decomposed image.

Since entropy is a measure of system structure [40], it is utilized in signal analysis and pattern recognition [41], [42]. In our study, we have incorporated seven entropy measures: Fuzzy [43], Kapur's (2 types) [42], [44], Maximum [45], Renyi's [46], Shannon's [40], and Yager's [47]. These measures are assistive in gauging the degree of randomness in the pixel distribution. Hence, the global texture pattern of an image can be extracted.

3) FEATURE APPENDING

Initially, bispectral features and entropies are stacked for every decomposed image and they are then appended together. This results in a high dimensional feature vector for each decomposed image. Finally, a different feature set is generated for BEMD and VMD decomposed images (i.e., feature set 1: using BEMD and feature set 2: using VMD). As a result, we have generated feature sets 1 and 2 of size 316×612 and 395×612 respectively.

B. GRAPH EMBEDDING AND CLASSIFICATION

Subspace learning is the most popular technique to reduce the dimension of the generated feature vector [48]. For the recognition or categorization task, the input should contain the rich structural details of the data points. In this respect, neighborhood preserving embedding (NPE) is proposed to maintain local information [49]. NPE addresses the "out of sample" problem and produces a linear projection matrix [49]. The basic steps for NPE are: i) the construction of a neighborhood graph G, ii) computation of the weight matrix, and iii) computation of the projection matrix. However, the discrimination capability of NPE is restricted by its unsupervised nature [50]. Since it uses the nonclass specific for neighborhood creation, the manifolds may overlap. Hence, in this work we have used supervised NPE to process new unknown data using class information [51]. The Euclidean distance matrix is generated using labeling information. Furthermore, the new G is constructed from the k–nearest neighbors of a data point x_i with x_j, if it shares the same label.

Let $X = \{x_i \in R^N\}$, where i=1,2,.....M, a projection matrix S can be found by solving,

$$\begin{aligned} &min\ S^T XLX^T S, \\ &\text{such that } S^T XX^T S = 1 \end{aligned} \tag{1}$$

where $L = (I - W)^T (I - W)$, and I and W are an identity and weight matrix, respectively [49].

Furthermore, the graph embedded features between groups are analyzed using analysis of variance (ANOVA) [52]. The obtained F-value is used to organize the features according to their weightage. These features provide for a successful classification of brain MRI. In the current study, the classifiers: linear discriminant analysis (LDA) and quadratic discriminant analysis (QDA) [53], [54], naive Bayes (NB) [55], [56], and support vector machine (SVM) [57], [58] are used. Figure 5 shows the necessary steps required to generate the feature vector, and its arrangement.

III. RESULTS

The algorithm is executed under a MATLAB environment without the need of a graphics processing unit. Initially, to maintain uniformity, images are resized to 128×128 pixels, and then two different feature sets are generated. During feature generation the IMFs are created using a sifting process and the IMF cost function is calculated by using $\varepsilon = 1 \times 10^{-8}$. The time required to compute the features based on BEMD is 8 seconds per image. The used parameters for VMD are: number of modes $K = 5$, bandwidth constraint $\alpha = 5000$ and tolerance for convergence is $K \times 10^{-6}$. The time required to compute the features based on VMD is 39 seconds per image. The SNPE is used for a total of five classes, and the feature size is reduced to a dimension of 30. The value $k = 5$ is *a priori* information used for graph construction. The resultant features are classified to categorize brain abnormality. To avoid the overfitting a 10-fold cross validation scheme is adopted and repeated for 10 times. In the current study multiclass categorization is treated as a multiple binary categorization task using one-against-all strategy. The statistical measures of specificity, sensitivity, and accuracy are used for evaluation. It is observed from the experimental results that the maximum classification accuracy (CA) obtained by BEMD is 84.47%, with a sensitivity and specificity of 99.62% and 75.9%, respectively, using 28 features, shown in Table 1.

The VMD results in a maximum CA of 90.68%, and a sensitivity and specificity of 99.43% and 87.95%, respectively, using 29 features, shown in Table 2. Performance of the combined features (BEMD+VMD) is shown in Table 3. Performance is reduced due to the combined features. Our results indicate that, the VMD based features (Table 2) have yielded the highest classification performance compared to the BEMD and BEMD+VMD features.

IV. DISCUSSION

In the present study, we have developed a system with the capacity to categorize brain abnormality. Initially, well-known decomposition techniques such as BEMD and

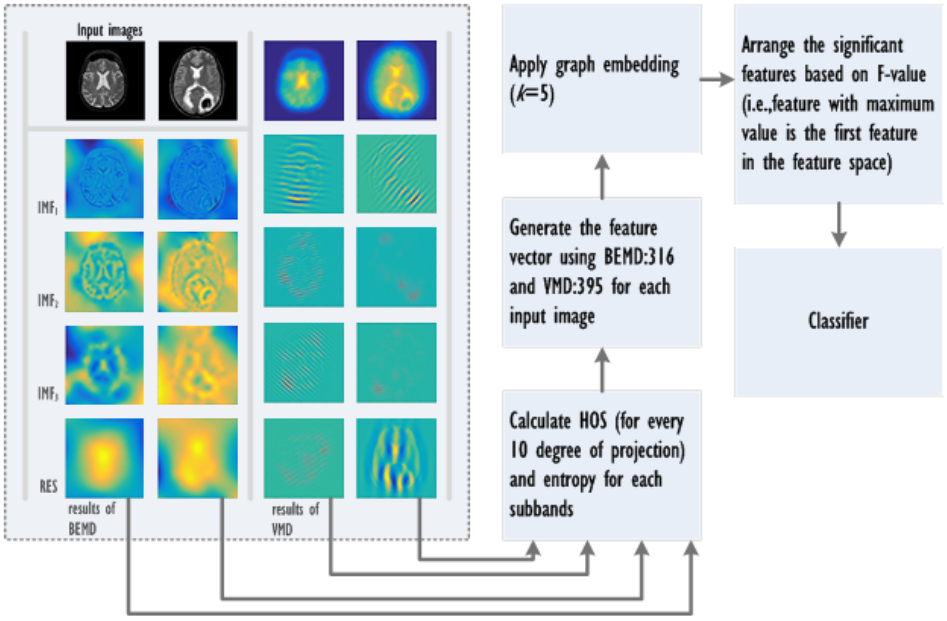

FIGURE 5. The representation of flow of proposed methodology.

TABLE 1. Multiclass categorization result using BEMD.

Classifier	#Features	CA (%)	Sensitivity (%)	Specificity (%)
LDA	29	67.15	94.13	67.46
QDA	29	66.50	90.17	83.13
NB	29	66.50	90.17	83.13
SVM:P1	28	61.11	85.44	92.77
SVM:P2	24	77.45	92.81	86.74
SVM:P3	**28**	**84.47**	**99.62**	**75.90**
SVM:RBF	8	68.30	94.89	71.08

* SVM:P1, P2, P3, and RBF are the polynomial 1,2,3, and radial basis function kernel respectively.

TABLE 2. Multiclass categorization result using VMD.

Classifier	#Features	CA (%)	Sensitivity (%)	Specificity (%)
LDA	30	67.97	95.65	78.31
QDA	30	61.92	93.76	92.77
NB	30	61.92	93.76	92.77
SVM:P1	30	64.86	87.33	98.79
SVM:P2	25	87.58	96.03	95.18
SVM:P3	**29**	**90.68**	**99.43**	**87.95**
SVM:RBF	10	80.88	99.05	86.74

TABLE 3. Multiclass categorization result using BEMD + VMD.

Classifier	#Features	CA (%)	Sensitivity (%)	Specificity (%)
LDA	27	74.18	96.40	77.10
QDA	29	64.86	92.43	85.54
NB	29	64.86	92.43	85.54
SVM:P1	28	68.13	88.84	96.38
SVM:P2	22	76.79	93.38	92.77
SVM:P3	**28**	**83.00**	**99.05**	**79.51**
SVM:RBF	9	79.41	97.35	87.95

VMD are used. Without decomposition, the method achieved a 75.49% accuracy using 30 features. The image with decomposition achieved improved results as compared to without decomposition. It is noted that VMD achieved a CA of 6.2% greater than BEMD (please refer to Figure 6). Methods such as Gabor filtering [59], and wavelet [60], curvelet [61], and shearlet [62] analysis, contain the various image components in several bands [31]. However, sparsity is addressed with the VMD component, hence revealing detailed brain structure.

Moreover, obscure brain features can be extracted using a bispectrum plot. HOS invariants are derived from the set of projected 1D data. Since RT is used to obtain the 1D data, the detailed inner structure of the brain is employed for the bispectral moments. Hence the extracted features exhibit the necessary local discriminatory shape characteristics of the brain. Thus HOS analysis is beneficial in nonlinearity identification. Along with these features, entropy features are also contributed, to obtain the pixel distribution of various portions of the brain. Feature reduction is carried out to further reduce HOS invariants and entropies, using threshold and SNPE. These graph embedded features are organized according to the F-value, which is generated from ANOVA, as shown in Table 4. The main intention of this step is to combine the most significant features for successful classification. The F-values of the first ten highly ranked features yielded high classification performance.

Graph embedding produces uncorrelated features by preserving large interclass separations. The class separability when using SNPE is evident using highly weighted features

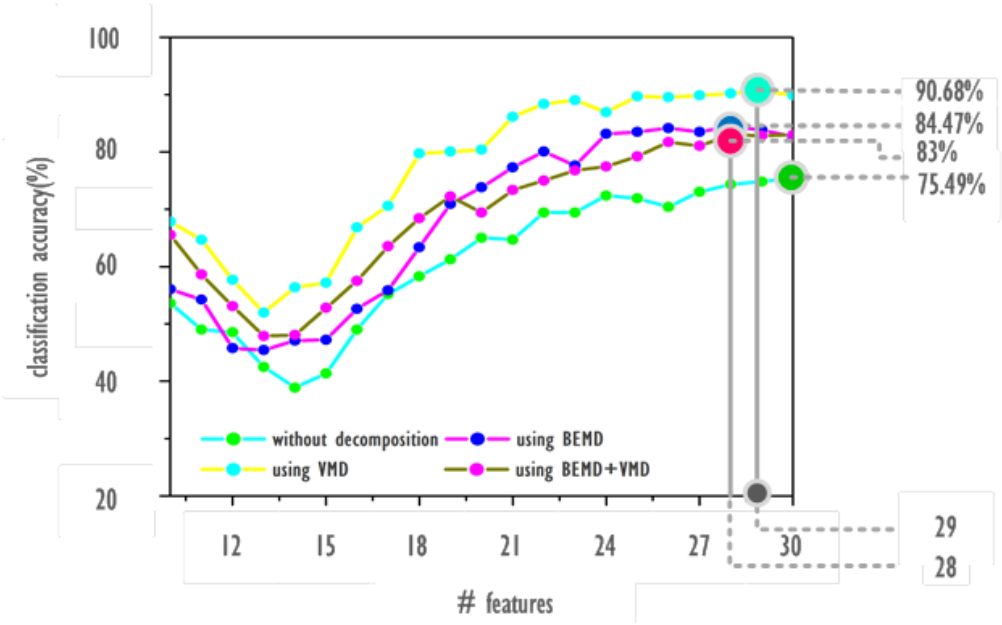

FIGURE 6. Graph of # features versus CA (%) for the 5-class problem using SVM classifier.

TABLE 4. Highly weighted features arrangement (only the starting ten features are shown).

Features	SNPE2	SNPE18	SNPE1	SNPE17	SNPE26	SNPE4	SNPE20	SNPE10	SNPE8	SNPE13
F-value	65.53	23.11	20.75	14.12	11.84	11.79	11.77	11.68	9.54	9.18

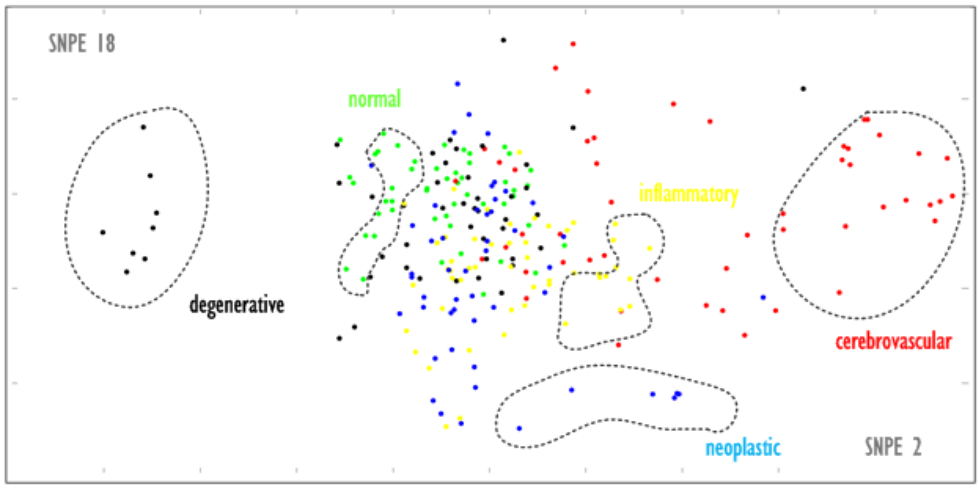

FIGURE 7. Plot of SNPE2 versus SNPE18 for the 5-class problem.

(Figure 7). Thus suitable information can be obtained for learning local architectural properties. Since it uses the same class samples for embedding, a small intra-class separation is produced. As a result, jumbled feature regions for foreign class neighbors are present (Figure 7). In order to investigate the within-class versus between-class structure, locality sensitive discriminant analysis [63] was implemented, with a CA of only 50% for 30 features. Hence, the SNPE is advantageous, although it uses local neighbors.

To determine the learning ability of SNPE, the entire problem is treated as a binary classification (class 0: normal and class 1: abnormal). The SNPE should be able to cluster the classes appropriately. In Figure 8 the satisfactory

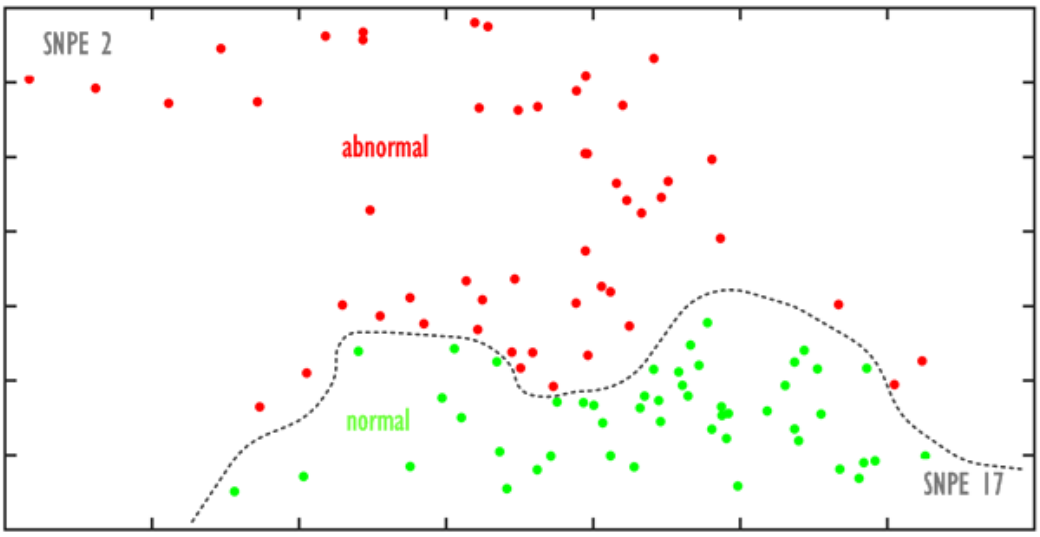

FIGURE 8. Plot of SNPE17 versus SNPE2 for the 2-class problem.

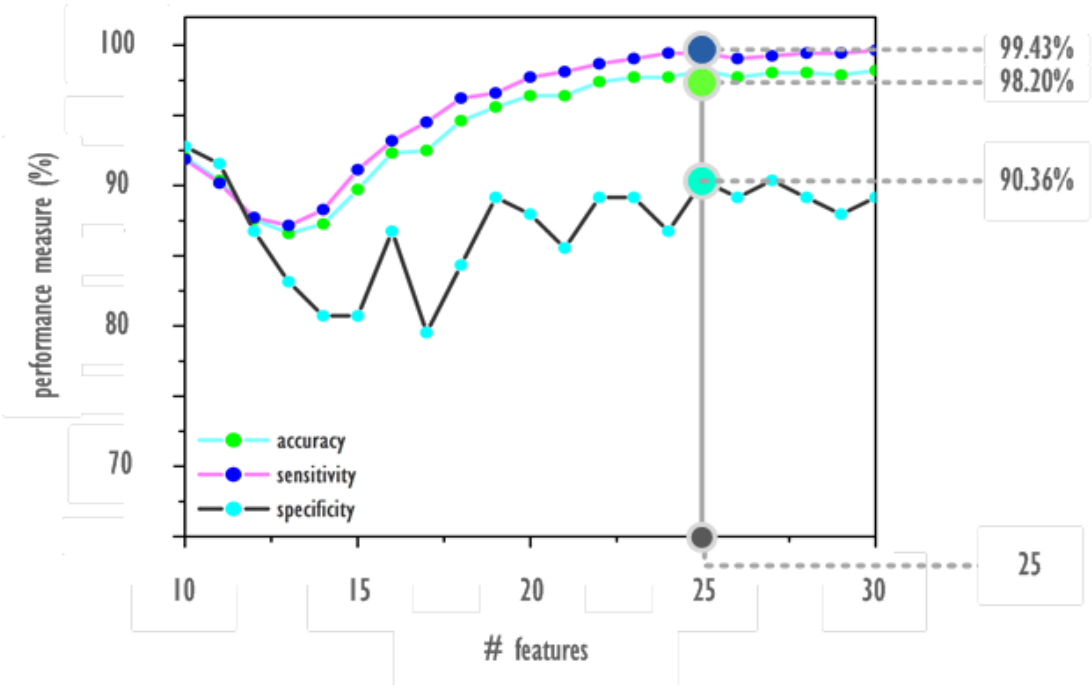

FIGURE 9. Graph of # features versus performance measure (%) for 2-class problem using SVM classifier.

discriminative power of SNPE for the 2-class problem is evident. Hence, using our proposed method, we have achieved highest CA of 98.20%, and sensitivity and specificity of 99.43% and 90.36% respectively, using only 25 features (please refer to Figure 9). Hence, this method is able to work with an imbalanced data distribution. In order to test the performance of combined features (BEMD + VMD), we have concatenated both features and tested the performance. The maximum accuracy is 83.00% for twenty-eight features. This confirms that VMD features are more discriminative than BEMD.

The methodologies adapted and the obtained results in the literature are concisely summarized in Table 5. It should be noted that our proposed method has achieved the best result for two classes, with a sensitivity reaching approximately 100%. To the best of our knowledge, the proposed method is the first to categorize four different brain pathologies using MRI.

The advantages of the proposed system are:

- The system addresses the 2-class as well as the 5-class problem effectively by studying the topological structure of the spectral feature space.

TABLE 5. Comparison using state-of-the-art approaches.

Paper	Methods	Classifiers/(dataset)	Accuracy (%) D:S	D:66	D:160	D:255
		2-class categorization				
[2]	DWT	SOM SVM (images:52= 6 + 46)	94 98			
[6]	DWT+PCA	ANN *k*-NN (images:70 =10 + 60)	95.70 98.60			
[7]	DWT+PCA	Back propagation neural network		100		
[8]	DWT+PCA	ACPSO with FNN			98.75	
[9]	DWT+PCA	SCABC with FNN		100		
[10]	DWT+PCA	KSVM with GRB			99.38	
[12]	DWT+PCA+LDA	Random forest				99.22
[13]	SWT+PCA	GEPSVM with RBF		100	100	99.41
[14]	Ripplet transform type-1	Least square SVM (LS-SVM)		100	100	99.39
[15]	FFE	Twin SVM		100	100	99.57
[16]	DTCWT + VE	Twin SVM		100	100	99.57
[17]	FFE	MLP + ARCBBO		100	99.75	99.53
[18]	Wavelet entropy	Naïve Bayes (images:64 = 18+46)	92.60			
[19]	Tsallis entropy	Fuzzy SVM		100	100	99.49
[20]	DWT	ADBRF		100	100	99.53
[25]	FDCT+PCA	LS-SVM		100	100	99.61
[26]	2DPCA + PCA+LDA	MDE-ELM		100	100	99.65
[28]	ST + Texture	PSO–SVM (images:612= 83 + 529)	97.38			
[77]	Pseudo Zernike moment	kernel SVM		100	99.75 ±0.32	99.45 ±0.38
[78]	AlexNet	(images: 291=resampled 114+177)	100			
[79]	ResNet34	(images: 613)	100			
[80]	FCEntF-II	kernel ELM		100	100	99.65
Proposed	**VMD+SNPE+ANOVA**	**SVM:P3 (images:612= 83 + 529)**	**98.20**			
		5-class categorization				
[80]	FCEntF-II	kernel ELM (images:200=40+160)	93			
Proposed	**VMD+SNPE+ANOVA**	**SVM:P3 (images:612= 83 + 529)**	**90.68**			

* images: total= normal + abnormal

- Reduced parameter tuning is needed to generate the graph embedded feature space.
- Since it uses a minimum number of features, computational demand is less. Hence the system may be used in a portable device.
- Since the system has a high degree of sensitivity, it can be implemented as a supportive tool for physicians, to begin early patient treatment.
- The paradigm can be generalized to address other types of pattern recognition and medical image analysis problems.

A. FUTURE DIRECTIONS

A recent development in the healthcare field is the introduction of Smart Health technology. This has enabled patients and their doctors to gain access to real-time data transfer, and it has assisted doctors and researchers in making the healthcare diagnostics sector more efficacious, by reducing the evaluation time and monetary costs. Smart Health has assisted patients to monitor their own health, and it enables them to gain a deeper knowledge and understanding concerning their personal situation and the disease management process. Recently, there has been an advance in healthcare technology, in that clinicians can acquire data even via a bed mattress or a wrist-wearable device, with direct parameter transfer [64]. A future application of the proposed CAD tool would be integration with a virtual cloud, to segregate brain MRI under the Smart Health context, as shown in Figure 10. Such MRI data would be acquired in-hospital, and the particular patient's data would then be uploaded to the virtual database. It would further be sent to the CAD network, preferably via CNN architecture at the cloud, for early prediction of

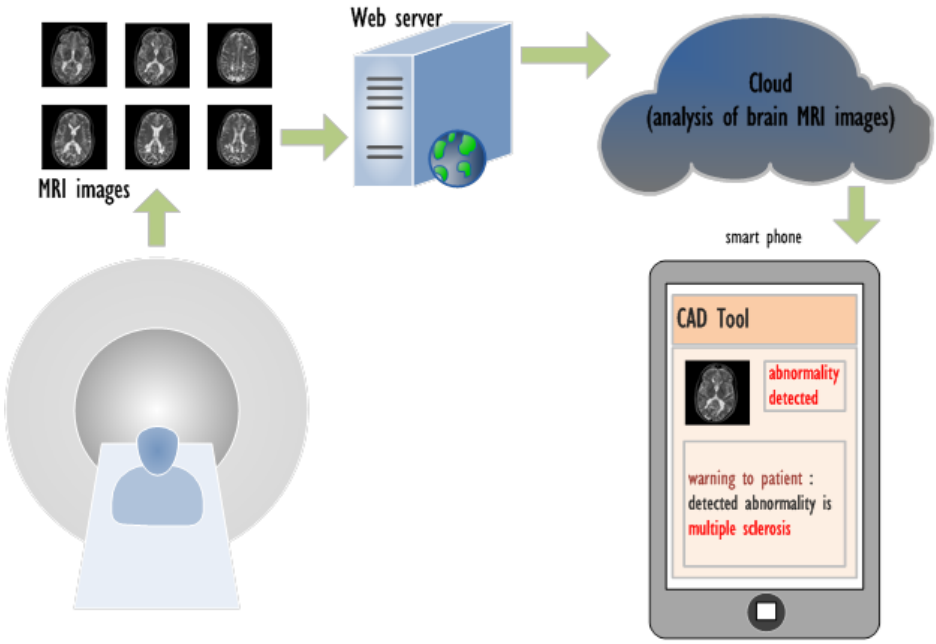

FIGURE 10. Integration of mobile application with virtual cloud analysis.

brain abnormality as CNN outperform most of existing techniques [65]–[72]. Once a prediction is made, a corresponding report would be sent to the patient via smart phone, as well as to any consultants, so that doctor and patient can coordinate further treatment modalities accordingly. A main intention behind this virtual cloud model would be to maintain a transparent doctor - patient relationship. Computational methods can also reduce the possibility of error or bias. The future implementation of the proposed cloud model may identify brain diseases at a very early stage.

V. CONCLUSION

Brain MR imagery has been utilized for automated categorization of brain disease into five different classes. From the obtained results, we conclude that a combination of VMD and bispectral feature techniques is useful to efficiently describe subtle image variation, which is useful for classification. The proposed methodology accurately identifies the presence or absence of pathology, which should be assistive to clinicians and researchers for diagnostics. A larger dataset including other pathologies may be used in future work to form an improved feature extraction and classification paradigm. Furthermore, integrating our system in a Smart Health application using CNN, a virtual cloud, and smart phone technology, can establish a transparent and minimal error data communication conduit between doctors and their patients.

REFERENCES

[1] *Harvard Medical School Data*. Accessed: Nov. 13, 2018. [Online]. Available: http://www.med.harvard.edu/AANLIB/

[2] L. M. Patnaik, S. Chaplot, and N. R. Jagannathan, "Classification of magnetic resonance brain images using wavelets as input to support vector machine and neural network," *Biomed. Signal Process. Control*, vol. 1, no. 1,pp. 86–92, 2006.

[3] *National Institute of Biomedical Imaging and Bioengineering*. Accessed: Aug. 24, 2018. [Online]. Available: https://www.nibib.nih.gov/science-education/science-topics/magnetic-resonance-imaging-mri

[4] K. Doi, "Computer-aided diagnosis in medical imaging: Historical review, current status and future potential," *Comput. Med. Imag. Graph*, vol. 31, nos. 4–5, pp. 198–211, 2007.

[5] E. S. A. El-Dahshan, H. M. Mohsen, K. Revett, and A. B. M. Salem, "Computer-aided diagnosis of human brain tumor through MRI: A survey and a new algorithm," *Expert Syst. Appl.*, vol. 41, no. 11, pp. 5526–5545, Sep. 2014.

[6] E. A. El-Dahshan, A. B. M. Salem, and T. H. Younis, "A hybrid technique for automatic MRI brain images classification," *Informatica*, vol. 54, no. 1, pp. 55–67, 2009.

[7] Y.-D. Zhang, Z. Dong, L. Wu, and S. Wang, "A hybrid method for MRI brain image classification," *Expert Syst. Appl.*, vol. 38, pp. 10049–10053, Aug. 2011.

[8] Y.-D. Zhang, S. Wang, and L. Wu, "A novel method for magnetic resonance brain image classification based on adaptive chaotic PSO," *Prog. Electromagn. Res.*, vol. 109, pp. 325–343, 2010.

[9] Y.-D. Zhang, L. Wu, and S. Wang, "Magnetic resonance brain image classification by an improved artificial bee colony algorithm," *Prog. Electromagn. Res.*, vol. 116, pp. 65–79, 2011.

[10] Y.-D. Zhang and L. Wu, "An MR brain images classifier via principal component analysis and kernel support vector machine," *Prog. Electromagn. Res.*, vol. 130, pp. 369–388, 2012.

[11] Y. Zhang, S. Wang, G. Ji, and Z. Dong, "An MR brain images classifier system via particle swarm optimization and kernel support vector machine," *Sci. World J.*, vol. 2013, Aug. 2013, Art. no. 130134.

[12] D. R. Nayak, R. Dash, and B. Majhi, "Classification of brain MR images using discrete wavelet transform and random forests," in *Proc. IEEE 5th Nat. Conf. Comput. Vis., Pattern Recognit., Image Process. Graph. (NCVPRIPG)*, Dec. 2015, pp. 1–4.

[13] Y. Zhang *et al.*, "Magnetic resonance brain image classification via stationary wavelet transform and generalized eigenvalue proximal support vector machine," *J. Med. Imag. Health Inf.*, vol. 5, no. 7, pp. 1395–1403, 2015.

[14] S. Das, M. Chowdhury, and K. Kundu, "Brain MR image classification using multiscale geometric analysis of ripplet," *Prog. Electromagn. Res.*, vol. 137, pp. 1–18, May 2013.

[15] S. Wang *et al.*, "Pathological brain detection by a novel image feature—Fractional Fourier entropy," *Entropy*, vol. 17, no. 12, pp. 8278–8296, 2015.

[16] S. Wang, S. Lu, Z. Dong, J. Yang, M. Yang, and Y. Zhang, "Dual-tree complex wavelet transform and twin support vector machine for pathological brain detection," *Appl. Sci.*, vol. 6, no. 6, p. 169, 2016.
[17] Y. Zhang, Y. Sun, P. Phillips, G. Liu, X. Zhou, and S. Wang, "A multilayer perceptron based smart pathological brain detection system by fractional Fourier entropy," *J. Med. Syst.*, vol. 40, p. 173, Jul. 2016.
[18] X. Zhou *et al.*, "Detection of pathological brain in MRI scanning based on wavelet-entropy and Naive Bayes classifier," in *Bioinformatics and Biomedical Engineering*. Cham, Switzerland: Springer, 2015, pp. 201–209.
[19] Y. Zhang *et al.*, "Pathological brain detection in MRI scanning by wavelet packet Tsallis entropy and fuzzy support vector machine," *SpringerPlus*, vol. 4, p. 716, Nov. 2015.
[20] D. R. Nayak, R. Dash, and B. Majhi, "Brain MR image classification using two-dimensional discrete wavelet transform and AdaBoost with random forests," *Neurocomputing*, vol. 177, pp. 188–197, Feb. 2016.
[21] Y. Zhang, S. Wang, P. Phillips, Z. Dong, G. Ji, and J. Yang, "Detection of Alzheimer's disease and mild cognitive impairment based on structural volumetric MR images using 3D-DWT and WTA-KSVM trained by PSOTVAC," *Biomed. Signal Process. Control* vol. 21, pp. 58–73, 2015.
[22] T. Li, W. Li, Y. Yang, and W. Zhang, "Classification of brain disease in magnetic resonance images using two-stage local feature fusion," *PLoS ONE*, vol. 12, no. 2, 2017, Art. no. e0171749. doi: 10.1371/journal.pone.0171749.
[23] N. V. Shree and T. N. R. Kumar, "Identification and classification of brain tumor MRI images with feature extraction using DWT and probabilistic neural network," *Brain Inform.*, vol. 5, no. 1, pp. 23–30, 2018.
[24] Virupakshappa and B. Amarapur, "Computer-aided diagnosis applied to MRI images of brain tumor using cognition based modified level set and optimized ANN classifier," *Multimedia Tools Appl.*, pp. 1–29, 2018. doi: 10.1007/s11042-018-6176-1.
[25] D. R. Nayak, R. Dash, and B. Majhi, "Pathological brain detection using curvelet features and least squares SVM," *Multimedia Tools Appl.*, vol. 77, pp. 3833–3856, Feb. 2018.
[26] D. R. Nayak, R. Dash, and B. Majhi, "An improved pathological brain detection system based on two-dimensional PCA and evolutionary extreme learning machine," *J. Med. Syst.*, vol. 42, p. 19, Jan. 2018. doi: 10.1007/s10916-017-0867-4.
[27] D. R. Nayak, R. Dash, and B. Majhi, "Discrete ripplet-II transform and modified PSO based improved evolutionary extreme learning machine for pathological brain detection," *Neurocomputing*, vol. 282, pp. 232–247, Mar. 2018.
[28] A. Gudigar, U. Raghavendra, T. R. San, E. J. Ciaccio, and U. R. Acharya, "Application of multiresolution analysis for automated detection of brain abnormality using MR images: A comparative study," *Future Gener. Comput. Syst.*, vol. 90, pp. 359–367, Jan. 2019.
[29] J. C. Nunes, Y. Bouaoune, E. Delechelle, O. Niang, and P. Bunel, "Image analysis by bidimensional empirical mode decomposition," *Image Vis. Comput.*, vol. 21, no. 12, pp. 1019–1026, 2003. doi: 10.1016/S0262-8856(03)00094-5.
[30] J. C. Nunes, S. Guyot, and E. Deléchelle, "Texture analysis based on local analysis of the bidimensional empirical mode decomposition," *Mach. Vis. Appl.*, vol. 16, no. 3, pp. 177–188, 2005.
[31] K. Dragomiretskiy and D. Zosso, "Two-dimensional variational mode decomposition," in *Proc. 10th Int. Conf. (EMMCVPR)*, 2015, pp. 197–208.
[32] T. Bülow and G. Sommer, "A novel approach to the 2D analytic signal," in *Computer Analysis of Images and Patterns*. Berlin, Germany: Springer, 1999, pp. 25–32.
[33] Y. Shao and M. Celenk, "Higher-order spectra (HOS) invariants for shape recognition," *Pattern Recognit.*, vol. 34, no. 11, pp. 2097–2113, 2001.
[34] K. C. Chua, V. Chandran, U. R. Acharya, and C. M. Lim, "Application of higher order statistics/spectra in biomedical signals—A review," *Med. Eng. Phys.*, vol. 32, pp. 679–689, Sep. 2010.
[35] A. Gudigar, S. Chokkadi, U. Raghavendra, and U. R. Acharya, "Local texture patterns for traffic sign recognition using higher order spectra," *Pattern Recognit. Lett.*, vol. 94, pp. 202–210, Jul. 2017.
[36] C. L. Nikias and M. R. Raghuveer, "Bispectrum estimation: A digital signal processing framework," *Proc. IEEE*, vol. 75, no. 7, pp. 869–891, Jul. 1987.
[37] S. R. Deans, "Hough transform from the radon transform," *IEEE Trans. Pattern Anal. Mach. Intell.*, vol. PAMI-3, no. 2, pp. 185–188, Mar. 1981.
[38] S. R. Deans, *The Radon Transform and Some of Its Applications*. New York, NY, USA: Wiley, 1983.
[39] K. C. Chua, V. Chandran, U. R. Acharya, and C. M. Lim, "Cardiac state diagnosis using higher order spectra of heart rate variability," *J. Med. Eng. Technol.*, vol. 32, no. 2, pp. 145–155, 2008.
[40] C. E. Shannon, "A mathematical theory of communication," *ACM SIGMOBILE Mobile Comput. Commun. Rev.*, vol. 5, no. 1, pp. 3–55, 2001.
[41] U. R. Acharya *et al.*, "Application of empirical mode decomposition (EMD) for automated identification of congestive heart failure using heart rate signals," *Neural Comput. Appl.*, vol. 28, no. 10, pp. 3073–3094, 2017.
[42] S. Ibrahim *et al.*, "Classification of diabetes maculopathy images using data-adaptive neuro-fuzzy inference classifier," *Med. Biol. Eng. Comput.*, vol. 53, no. 12, pp. 1345–1360, 2015.
[43] W. Chen, Z. Wang, H. Xie, and W. Yu, "Characterization of surface EMG signal based on fuzzy entropy," *IEEE Trans. Neural Syst. Rehabil. Eng.*, vol. 15, no. 2, pp. 266–272, Jun. 2007.
[44] J. Kapur, "Information of order α and type β," *Proc. Indian Acad. Sci.*, vol. 68, pp. 65–75, Aug. 1968.
[45] P.-Y. Yin, "Maximum entropy-based optimal threshold selection using deterministic reinforcement learning with controlled randomization," *Signal Process.*, vol. 82, no. 7, pp. 993–1006, 2002.
[46] A. Rényi, "On measures of entropy and information," in *Proc. 4th Berkeley Symp. Math., Statist. Probab.*, 1960, pp. 547–561.
[47] M. Ghosh, C. Chakraborty, and A. K. Ray, "Yager's measure based fuzzy divergence for microscopic color image segmentation," in *Proc. Indian Conf. Med. Inform. Telemedicine*, Kharagpur, India, 2013, pp. 13–16.
[48] P. N. Belhumeur, J. P. Hespanha, and D. Kriegman, "Eigenfaces vs. Fisherfaces: Recognition using class specific linear projection," *IEEE Trans. Pattern Anal. Mach. Intell.*, vol. 19, no. 7, pp. 711–720, Jul. 1997.
[49] X. He, D. Cai, S. Yan, and H.-J. Zhang, "Neighborhood preserving embedding," in *Proc. 10th IEEE Int. Conf. Comput. Vis.*, Oct. 2005, pp. 1208–1213.
[50] P. Y. Han, A. T. B. Jin, and F. S. Abas, "Neighbourhood preserving discriminant embedding in face recognition," *J. Vis. Commun. Image Represent.*, vol. 20, pp. 532–542, Nov. 2009.
[51] X. Zeng and S. Luo, "A supervised subspace learning algorithm: Supervised neighborhood preserving embedding," in *Proc. 3rd Int. Conf. Adv. Data Mining Appl.*, 2007, pp. 81–88.
[52] A. Gelman, "Analysis of variance—Why it is more important than ever," *Ann. Statist.*, vol. 33, no. 1, pp. 1–53, 2005.
[53] T. M. Cover, "Geometrical and statistical properties of systems of linear inequalities with applications in pattern recognition," *IEEE Trans. Electron. Comput.*, vol. EC-14, no. 3, pp. 326–334, Jun. 1965.
[54] R. A. Fisher, "The use of multiple measurements in taxonomic problems," *Ann. Eugenics*, vol. 7, no. 2, pp. 179–188, 1936. [Online]. Available: https://digital.library.adelaide.edu.au/dspace/handle/2440/15227
[55] T. Hastie, R. Tibshirani, and J. Friedman, *The Elements of Statistical Learning*, 2nd ed. New York, NY, USA: Springer, 2008.
[56] C. D. Manning, P. Raghavan, and H. Schütze, *Introduction to Information Retrieval*. New York, NY, USA: Cambridge Univ. Press, 2008.
[57] V. Vapnik, "*The Nature of Statistical Learning Theory*. New York, NY, USA: Springer-Verlag, 1995.
[58] C. J. C. Burges, "A tutorial on support vector machines for pattern recognition," *Data Mining Knowl. Discovery*, vol. 2, no. 2, pp. 121–167, 1998.
[59] T. S. Lee, "Image representation using 2D Gabor wavelets," *IEEE Trans. Pattern Anal. Mach. Intell.*, vol. 18, no. 10, pp. 959–971, Oct. 1996.
[60] S. G. Mallat, "A theory for multiresolution signal decomposition: The wavelet representation," *IEEE Trans. Pattern Anal. Mach. Intell.*, vol. 11, no. 7, pp. 674–693, Jul. 1989.
[61] E. J. Candes and D. L. Donoho, "Curvelets: A surprisingly effective nonadaptive representation for objects with edges," in *Proc. Curve Surf. Fitting*, 1999, pp. 105–120.
[62] K. Guo and D. Labate, "Optimally sparse multidimensional representation using shearlets," *SIAM J. Math. Anal.*, vol. 39, no. 1, pp. 298–318, 2007.
[63] D. Cai, X. He, K. Zhou, J. Han, and H. Bao, "Locality sensitive discriminant analysis," in *Proc. 20th Int. Joint Conf. Artif. Intell.*, New Delhi, India, 2007, pp. 708–713.
[64] R. K. Kher, "Mobile and E-healthcare: Recent trends and future directions," *J. Health Med. Econ.*, vol. 2, no. 3, pp. 1–8, 2016.
[65] U. Raghavendra, N. S. Bhat, A. Gudigar, and U. R. Acharya, "Automated system for the detection of thoracolumbar fractures using a CNN architecture," *Future Gener. Comput. Syst.*, vol. 85, pp. 184–189, Aug. 2018.
[66] U. Raghavendra, H. Fujita, S. V. Bhandary, A. Gudigar, J. H. Tan, and U. R. Acharya, "Deep convolution neural network for accurate diagnosis of glaucoma using digital fundus images," *Inf. Sci.*, vol. 441, pp. 41–49, May 2018.

[67] U. R. Acharya *et al.*, "Automated identification of shockable and non-shockable life-threatening ventricular arrhythmias using convolutional neural network," *Future Gener. Comput. Syst.*, vol. 79, pp. 952–959, Feb. 2018.
[68] J. H. Tan *et al.*, "Age-related macular degeneration detection using deep convolutional neural network," *Future Gener. Comput. Syst.*, vol. 8, pp. 127–135, Oct. 2018.
[69] U. R. Acharya *et al.*, "A deep convolutional neural network model to classify heartbeats," *Comput. Biol. Med.*, vol. 89, pp. 389–396, Oct. 2017.
[70] J. H. Tan *et al.*, "Application of stacked convolutional and long short-term memory network for accurate identification of CAD ECG signals," *Comput. Biol. Med.*, vol. 94, pp. 19–26, Mar. 2018.
[71] S. L. Oh, E. Y. k. Ng, R. S. Tan, and U. R. Acharya, "Automated diagnosis of arrhythmia using combination of CNN and LSTM techniques with variable length heart beats," *Comput. Biol. Med.*, vol. 102, no. 1, pp. 278–287, Nov. 2018.
[72] Ö. Yildirim, P. Plawiak, R.-S. Tan, and U. R. Acharya, "Arrhythmia detection using deep convolutional neural network with long duration ECG signals," *Comput. Biol. Med.*, vol. 102, no. 1, pp. 411–420, Nov. 2018.
[73] P. P. R. Filho, E. De S. Rebouças, L. B. Marinho, R. M. Sarmento, J. M. R. S. Tavares, and V. H. C. de Albuquerque, "Analysis of human tissue densities: A new approach to extract features from medical images," *Pattern Recognit. Lett.*, vol. 94, pp. 211–218, Jul. 2017.
[74] E. de S. Rebouças, R. C. P. Marques, A. M. Braga, S. A. F. Oliveira, V. H. C. de Albuquerque, and P. P. R. Filho, "New level set approach based on Parzen estimation for stroke segmentation in skull CT images," *Soft Comput.*, pp. 1–22, Aug. 2018. doi: 10.1007/s00500-018-3491-4.
[75] N. Arunkumar, M. A. Mohammed, S. A. Mostafa, D. A. Ibrahim, J. J. P. C. Rodrigues, and V. H. de Albuquerque, "Fully automatic model-based segmentation and classification approach for MRI brain tumor using artificial neural networks," in *Concurrency and Computation: Practice and Experience*. Hoboken, NJ, USA: Wiley, 2018. doi: 10.1002/cpe.4962.
[76] N. Arunkumar *et al.*, "*K*-means clustering and neural network for object detecting and identifying abnormality of brain tumor," *Soft Comput.*, pp. 1–14, 2018. doi: 10.1007/s00500-018-3618-7.
[77] Y.-D. Zhang, Y. Jiang, W. Zhu, S. Lu, and G. Zhao, "Exploring a smart pathological brain detection method on pseudo Zernike moment," *Multimedia Tools Appl.*, vol. 77, pp. 22589–22604, Sep. 2018.
[78] S. Lu, Z. Lu, and Y.-D. Zhang, "Pathological brain detection based on AlexNet and transfer learning," *J. Comput. Sci.*, vol. 30, pp. 41–47, Jan. 2019.
[79] M. Talo, U. B. Baloglu, Ö. Yıldırım, and U. R. Acharya, "Application of deep transfer learning for automated brain abnormality classification using MR images," *Cogn. Syst. Res.*, vol. 54, pp. 176–188, May 2019.
[80] D. R. Nayak, R. Dash, X. Chang, B. Majhi, and S. Bakshi, "Automated diagnosis of pathological brain using fast curvelet entropy features," *IEEE Trans. Sustain. Comput.*, to be published. doi: 10.1109/TSUSC.2018.2883822.

ANJAN GUDIGAR received the Ph.D. degree from the Manipal Academy of Higher Education, India. He is currently a Faculty with the Department of Instrumentation and Control Engineering, Manipal Institute of Technology, Manipal, India. He has published several research papers in international conferences and journals. His research interests include image processing, medical image analysis, and pattern recognition.

U. RAGHAVENDRA received the Ph.D. degree from the Manipal Academy of Higher Education, India. He is currently a Faculty with the Department of Instrumentation and Control Engineering, Manipal Institute of Technology, Manipal, India. He has published several papers in refereed international SCI-IF journals and international conference proceedings. He has a patent to his credit and received an invention award from Intellectual Ventures, USA, for his innovations in 2014. His current research interests include 3D computer vision, image processing, and medical image analysis.

EDWARD J. CIACCIO received the Ph.D. degree from Rutgers University. He is currently a Senior Research Scientist with the Department of Medicine, Division of Cardiology, and also with the Celiac Disease Center, Columbia University, and also an Honorary Principal Research Fellow with the Department of Medicine, Division of Cardiology, Imperial College London. He has published more than 100 peer-reviewed articles on such topics as biomedical signal processing of heart electrograms, and image processing of villous atrophy in celiac disease patients. In computational biology, he has developed biophysical models of activation wavefront propagation for ventricular tachycardia and for atrial fibrillation. His work received a Paper of the Year Award from *Heart Rhythm* journal, in 2008. He is Editor-In-Chief of the journals *Computers in Biology and Medicine* and *Informatics in Medicine Unlocked*. He was a Keynote Speaker at the International Conference on Biomedical Engineering and Biotechnology, from 2013 to 2015, and the Innovation in Medicine and Healthcare, in 2014. He was a Faculty Speaker at the 1st Annual International Symposium on Ventricular Arrhythmias 2006, Atrial Signals 2015, the 13th Annual Congress of the European Cardiac Arrhythmia Society 2017, and Boston Signals Summit 2018.

N. ARUNKUMAR received the B.E. and M.E. degrees in electronics and communication engineering with a specialization in biomedical engineering. He has a strong academic teaching and research experience more than 11 years in SASTRA University, India. He is appreciated for his innovative research oriented teaching related practical life experiences to the principles of engineering. He is active in research.

ENAS ABDULHAY is currently a Faculty Member with the Department of Biomedical Engineering, Faculty of Engineering, Jordan University of Science and Technology, Irbid, Jordan. She has published several research papers in biomedical engineering and is active in research.

U. RAJENDRA ACHARYA received the Ph.D. degree from the National Institute of Technology Karnataka, Surathkal, India, and the D.Eng. degree from Chiba University, Japan. He is currently a Senior Faculty Member with Ngee Ann Polytechnic, Singapore. He is also an Adjunct Professor with Taylor's University, Malaysia, an Adjunct Faculty with the Singapore Institute of Technology–University of Glasgow, Singapore, and an Associate Faculty with the Singapore University of Social Sciences, Singapore. He has published more than 400 papers, in refereed international SCI-IF journals (345), international conference proceedings (42), books (17) with more than 19,900 citations in Google Scholar (with h-index of 73), and ResearchGate RG Score of 47.05. He is ranked in the top 1% of the Highly Cited Researchers for the last three consecutive years (2016, 2017, and 2018) in computer science according to the Essential Science Indicators of Thomson. He has worked on various funded projects, with grants worth more than 2 million SGD. He has three patents and an editorial board member of many journals. His research interests include biomedical signal processing, biomedical imaging, data mining, visualization and biophysics for better healthcare design, delivery, and therapy. He has served as a Guest Editor for many journals.